Food & Function

Accepted Manuscript

This article can be cited before page numbers have been issued, to do this please use: Y. Huang, D. Lu, H. Liu, S. Liu, S. Jiang, G. Pang and Y. Liu, *Food Funct.*, 2019, DOI: 10.1039/C8FO02522C.

ROYAL SOCIETY OF CHEMISTRY

rsc.li/food-function

ROYAL SOCIETY OF CHEMISTRY View Article Online
DOI: 10.1039/C8FO02522C

Journal Name

ARTICLE

Preliminary research on receptor-ligand recognition mechanism of umami by hT1R1 biosensor

Received 00th January 20xx,
Accepted 00th January 20xx

DOI: 10.1039/x0xx00000x

www.rsc.org/

Yulin Huang‡[a], Dingqiang Lu‡[b], Hai Liu[a], Suyao Liu[a], Shui Jiang[c], Guang-chang Pang*[b], Yuan Liu*[c]

The aim of this work was to determine the interaction between human umami receptor hT1R1 and the ligand, at the same time to avoid "Cross-Talking" among various signal pathways in cells. The hT1R1 was modified and mounted to a signal amplification system on glassy carbon electrode surface, and the response current to four umami ligands (sodium glutamate (MSG), disodium inosinate (IMP), disodium guanylate (GMP), and disodium succinate (SUC)) was measured. The allosteric constants of receptor-ligand interaction were calculated by the method of sensing kinetics, and the results indicated that the ability of hT1R1 sensing to four ligands were as follows: GMP > MSG > IMP > SUC. After the analysis of molecular structure and simulation through molecular docking model, we found that hT1R1 was essentially a recognition receptor for “nitrogen” signal in the body, and it might recognize the umami substance through its amino group. The new research method developed in this paper showed promising application in the mechanism study of signal transduction and drug screening.

1. Introduction

Umami receptor belongs to the class C of G protein-coupled receptors (GPCRs), and two types of receptor have been identified: heterodimers T1R1/T1R3 and metabotropic glutamate receptors (mGluRs)[1, 2]. It has been confirmed that T1R1/T1R3 is not only present in mammalian taste buds, but also in other tissues and organs[3-6]. This discovery implies that T1R1/T1R3 may play a special role in mammals.

Although the umami receptor T1R1/T1R3 and the sweet receptor T1R2/T1R3 share a T1R3, they recognize different taste compounds, which is due to the structural difference in ligand recognition sites (Venus flytrap (VFT)) present at T1R1 and T1R2[7]. Feng (2008) verified this by chimeric receptor model, and molecular dynamic simulation to find that the recognition site of L-glutamic acid was located inside the VFT region and close to the hinge region, while the disodium inosinate (IMP) was located the opening area of the VFT, and the VFT domain played a decisive role in umami taste synergistic[8]; In addition, Dang (2014) discovered the receptor-ligand interaction was a positive allosteric regulatory mechanism through homologous molecular modeling[9]. The ligand bound to the VFT outer vestibular site of the receptor and maintained a stable state for further recognition; In addition, Yu (2017) further showed the interaction was a hydrogen-bonding in nature when the ligands were caught by T1R1[10]. Using molecular docking technology to research receptor-ligand binding has made great progress in the past decades, but it was still unclear how T1R1 specifically recognized umami substances and showed a difference in sensitivity.

The common methods for studying receptor-ligand binding include surface plasmon resonance (SPR) and some biosensors based on taste component detection, most of those were detected by measuring the adsorption-dissociation rules of the

[a] College of Food Science and Technology, Shanghai Ocean University, Shanghai 201306, PR China.
[b] College of Biotechnology and Food Science, Tianjin University of Commerce, Tianjin 300134, PR China.
[c] Department of Food Science and Technology, School of Agriculture and Biology, Shanghai Jiao Tong University, Shanghai 200240, China.
‡ Contributed equally.

receptor-ligand[11-14]. However, the key role of the 7-transmembrane domain of the receptor in activating signalling pathways was neglected, because signal transmission was a chain reaction from intracellular to extracellular[15]. In addition, some studies have proposed biosensors based on whole animals. For example, the microelectrode array was coupled to the rat's taste cortex for a long time by brain-computer interface (BMI) technology to record the extracellular potential of a group of neurons, and the purpose of detecting bitter substances using a rodent taste system was realized[16, 17]. Although a highly sensitive taste detection platform was constructed, there are many unresolved problems in the physiological basis of the rodent's taste system. Therefore, it cannot be used as an indicator to judge the degree of taste of human beings.

Due to the high selectivity and sensitivity, electrochemical biosensors have been widely applied to detect various substances[18]. Thiopurine (Thi), Chitosan (Chit) and Horseradish peroxidase (HRP) acted by simulating cascade amplification in the process of biosignal transmission. As a typical oxidoreductase, HRP enables direct transfer of electrons between two delivery media[19-23], and hT1R1 was adsorbed and immobilized on the system by gold nanoparticles(AuNPs)[24]. The detection system avoided the effect of "Cross-Talking" among signal amplification pathways within live cells，and has been proven to enjoy good detection performances[19-23]. The detection system was able to directly study on human receptor-ligand interaction mechanisms.

2. Experimental

2.1 Acquisition of hT1R1 protein

Human embryonic kidney 293 (HEK-293) cells were cultured in Dulbecco's Modified Eagle Medium (DMEM), supplemented with 10% fetal bovine serum and 1% penicillin-streptomycin (Gibco), at 37 ℃ under 5% CO_2[25]. The cells were transfected with the mammalian expression vector pCMV6ENTRY containing human TAS1R1 using Lipofectamine2000 (Invitrogen) according to the manufacturer's instructions. After the transfection, the cells were cultured in an incubator for 48 hours, the T1R protein was extracted, and confirmed by Western blot analysis.

2.2 Fabrication of hT1R1 electrochemical biosensor

Under specific conditions, 6 microliters solution of AuNPs, Thi, Chit, HRP were added dropwise to the bare electrode respectively at 4 ℃[26]. After the current substance was completely dried, the next substance can be dripped in. Receptor modification was self-assembled for 24 hours by immersing the electrode in 1 mg/ml hT1R1 solution. Finally, a double-layer gold nanoparticle sensor was fabricated, the linkage of the signal during the generation and amplification process from extracellular to intracellular was mimicked by the membrane structure of the multi-layered material (**Fig 1**). In our previous related studies, the sensor demonstrated the assembly process had a good detection performance[22, 24].

2.3 Detection of umami substances

Under the three-electrode system, a prepared biosensor (glassy carbon electrode) was used as the working electrode, the Ag/Ag Cl electrode and platinum wire electrode were used as the reference electrode and counter electrode. Ultrapure water containing 10 mM H_2O_2 was used as a blank control. Current-time measurement (I - t) was used to determine the response current of the sensor of four ligands at different concentrations, the optimized potential was chosen to be -0.38V and the response time was 90 seconds. The change of the response currents was calculated by the equation (1)，and worked as the detection index[27]. Where the I_0 was the steady-state current values of determination ultrapure water, and I_1 was detected umami substances, at the same time point.

$$\Delta I\ \% = \frac{I_0 - I_1}{I_0} \times 100 \qquad (1)$$

2.4 Recognition mechanism analysis of receptor-ligand

Refer to the evaluation method of receptor sensing kinetics, the allosteric constant was derived to quantitatively describe the receptor-ligand interaction. Allosteric constants (K_a) of hT1R1 to MSG, IMP, GMP and SUC were calculated, which was defined as: the concentration of ligand at half of the maximum output signals of cells. The interaction regulations between the allosteric constant and the ligand molecule structure was analysed, and verified by molecular docking experiment.

Fig. 1 Schematic diagram of electrode assembly process and detection principle. (a) Electrode assembly process. (b) Principle of detection.

3. Results and discussion

3.1 Expression of human taste receptors(hT1R1) and construction of gold nanoparticles

Fig 2a shows the western blot (WB) analysis result of hT1R1 expressed by HEK 293T cells by using rabbit anti-hT1R1 as primary antibodies and goat anti-rabbit secondary antibodies, which were blocked with skimmed milk powder. The negative control was the first lane and no bands were observed. The expression of hT1R1 lanes were in lanes 2 and 3, respectively, and a clear band appeared at 75 kD. Therefore, the hT1R1 was successfully expressed in HEK293T cells, and used for fabricating biosensor after the processes of extraction and purification.

The results of the AuNPs solution at a scanning electron microscope with a resolution of 20nm and 10nm are shown in **Fig 2(b, c)**. **Fig. 2 (b)** is a scanning electron microscope (SEM) image of AuNPs colloidal solution at the resolution level of 20 nm. It can be clearly observed that AuNPs are uniformly dispersed and spherically round. And **Fig 2 (c)** is another SEM image at the resolution level of 10 nm with even AuNPs particle size in 10 nm, indicating that the prepared AuNPs are suitable for the fabrication of biosensors.

Fig. 2 (a) Immunoblot analysis of the receptor protein expressed by HEK293; (b) scanning electron microscopy (SEM) image of AuNPs particles at 20 nm resolution; (C)

scanning electron microscopy (SEM) image of AuNPs particles at 10 nm resolution.

3.2 The fabrication of biosensor

The characterization results of cyclic voltammetry (scanning range -0.1 ~ 0.6 V, scan rate 50 mV s^{-1}) are shown in **Fig 3(a)**. Since the Chit film hinders the transfer of electrons on the surface of the electrode, the peak current of bare electrode (curve a) was decreased compared with the curve b (modified 0.5% chitosan electrode); After modified AuNPs (curve c), the main roles of AuNPs are to accelerate electron transfer and adsorb receptor proteins. Therefore, the peak current of curve c increases relative to curve b; And then, the hT1R1 was modified on the surface of the electrode, the redox peak current of the curve d decreases compared with the curve c. This is because the receptor hinders the electron transfer, indicating that the receptor has been assembled successfully; The peak value of curve e (Thi/Chit complex) was larger than d, because the electron transfer ability of Thi was stronger than the electron blocking effect of Chit; Compared to curve e, the peak current value of curve f (AuNPs /HRP complex) was increased further, because the promotion effect of electron transfer of AuNPs was better than the steric factor of HRP; After modified hT1R1 again, the peak current of curve g was significantly reduced compared with curve f, which illustrates that the second layer hT1R1 was assembled successfully; Finally, after dropped BSA, the peak current of curve h was reduced more, which indicates that BSA had closed the non-specific locus on the electrode surface.

In order to more directly characterize the receptor assembled to the electrode surface, this study characterized self-absorption AuNPs surfaces, re-adsorption hT1R1 surfaces, BSA closed electrode surface and binding ligand surfaces (the electrode assembly last four steps in Fig. 3(a)) in two-dimensional images using atomic force microscopy (AFM) by tapping mode as shown in **Fig. 3**. And their related parameters were also shown in **Table 1**. From **Fig. 3b**, we learned that the uniform and dense small sphere particles were formed in the glassy carbon electrode with little aggregation after AuNPs adsorption. The surface roughness Ra of the film was increased from 4.43 to 7.17 nm, because the spherical AuNPs uniformly covers the smooth film surface. From **Fig. 3c**, the electrode surface had an aggregation with lots spots after AuNPs adsorbs hT1R1, and this may be because AuNPs plays an adsorption role in receptor protein. Finally, the surface of the electrode became gentle after blocking the gold nanoparticles of the unadsorbed hT1R1 on the electrode surface (**Fig. 3d**), and Ra drops decreased to one third of the original. Ra and peak depth were both multiplied, when the hT1R1-sensor assembly was completed and placed in a MSG solution for 15 minutes at 37 °C (**Fig. 3e**). This indicates that a specific reaction occurred between the receptor and ligand, and a large amount of complex was formed.

Fig. 3(a) Characterized electrode in modifying process by cyclic voltammetry: a - h represent GCE, Chit-GCE, AuNPs -Chit-GCE, hT1R1-AuNPs-Chit-GCE, Thi/Chi/hT1R1-AuNPs-Chit-GCE, HRP/Nano-Au-Thi/Chit-1R1-Chit-GCE, hT1R1-HRP/ AuNPs -Thi/Chit-hT1R1-AuNPs-Chit-GCE and BSA-hT1R1-HRP/ AuNPs -Thi/Chit-hT1R1-AuNPs -Chit-GCE, respectively; (b) The self-absorption AuNPs surfaces characterized by AFM; (c) The re-adsorption hT1R1 surfaces characterized by AFM; (d) BSA closed electrode surface characterized by AFM; (e) The binding ligand surfaces characterized by AFM.

3.3 Allosteric constant

When the umami substances were caught by hT1R1 on the surface of glassy carbon electrode, the response signal was affected by changes of receptor conformation, and these output signals can be inducted with electrochemical workstations. Therefore, when the prepared sensor was placed in a test solution containing a ligand (MSG, etc.), the response current would show a significant change range relative to the ligand-free detection base. The line graphs were plotted with lg (C) as X-axis and ΔI% as Y-axis, and the results showed in **Fig 4**. There are good linear relationships between ΔI % with the lg (C) in the range of $10^{-14} \sim 10^{-12}$ mol/L, respectively.

Fig. 4 Current response values of umami substances in the detection range (lg C): a, b, c, d represent MSG, IMP, GMP and SUC, respectively.

According to receptor-ligand kinetics and our previous reports, the biological effects of receptor-ligand interactions are consistent with the enzymatic reaction kinetics curve[27, 28]. Therefore, the hyperbolic curve fitting was performed in the concentration ranges mentioned above. The line graphs were replotted with the further partitioned concentration as X-axis and ΔI % as Y-axis (**Fig 5**). The fitting formulae are as follows:

$$\Delta I_{MSG}\% = 49.01877 \times C/(0.74223 + C) \ (R^2=0.9822)$$

$$\Delta I_{IMP}\% = 67.76482 \times C/(1.54392 + C) \ (R^2=0.9691)$$

$$\Delta I_{GMP}\% = 40.77952 \times C/(0.55467 + C) \ (R^2=0.9893)$$

$$\Delta I_{SUC}\% = 56.79040 \times C/(2.43424 + C) \ (R^2=0.9800)$$

According to the Lineweaver-Burk Equation, the reciprocal of the ligands concentration (1/C) was regarded as the X axis, and the reciprocal of ΔI% (1/ΔI%) was plotted as the Y axis. The results showed a good linear relationship (R^2 >0.95) between 1/ΔI% with 1/C and the linear regression equations are as follows:

$$\frac{1}{\Delta I_{MSG}\%} = 1.513 \times 10^{-16}\frac{1}{C} + 0.0203 \ (R^2=0.9603)$$

$$\frac{1}{\Delta I_{IMP}\%} = 2.695 \times 10^{-16}\frac{1}{C} + 0.0141 \ (R^2=0.9759)$$

$$\frac{1}{\Delta I_{GMP}\%} = 1.333 \times 10^{-16}\frac{1}{C} + 0.0245 \ (R^2=0.9786)$$

$$\frac{1}{\Delta I_{SUC}\%} = 4.013 \times 10^{-16}\frac{1}{C} + 0.0178 \ (R^2=0.9899)$$

Fig. 5 Fitting graph of the interaction between umami receptors and ligands and the embedded diagram represent double curve fitting. The a, b, c, d represent the ligand of MSG, IMP, GMP, SUC, respectively.

Allosteric constants (K_a) of hT1R1 to MSG, IMP, GMP and SUC were calculated by above formula, which was defined as: the concentration of ligand at half of the maximum output signals of cells. The K_a of the interaction of MSG, IMP, GMP, SUC were $K_{MSG}=7.420\times10^{-16}$ mol/L, $K_{IMP}=1.899\times10^{-15}$ mol/L, $K_{GMP}=5.449\times10^{-16}$ mol/L, $K_{SUC}=2.251\times10^{-15}$ mol/L. The K_a was

similar to K_m (Mie equation), and the smaller the K_a value was, the higher efficiency of the signal output generated by the receptor-ligand interaction. It demonstrated the sensitivity of hT1R1 for four umami substances as follows: GMP > MSG > IMP > SUC. Therefore, the downstream signal intensity produced by binding of the receptor to the ligand could be compared by the K_a value. Meanwhile, the detection limit (LODs) of the hT1R1-sensor were calculated (S/N = 3) for different umami compounds, and the LODs (1.5pM, 0.88pM, 2.3pM and 0.86pM for MSG, IMP, GMP and SUC respectively) were lower than others studies but unacceptable in applications[29-32]. What's more, at a very low concentration, the hT1R1-sensor could still give a response signal, indicating that hT1R1 had an excellent recognition and sensing effect to each ligand.

3.4 Recognition mechanism of umami receptor

The ligands of MSG and GMP have amino groups in their molecular structures, however, the IMP and SUC do not (**Fig 6. Inline graph**). In addition, MSG and GMP have a lower K_a value than IMP and SUC. It suggests that the amino group may be a group recognized by hT1R1 for the umami ligand. We further analysed the two amino-containing ligands (MSG and GMP), which showed that the smaller the K_a value, the higher the nitrogen content.

To confirm the characteristic of this interaction, homology modeling was applied to construct the hT1R1/T1R3, and then 5x2m.1 (pdb) was selected as template protein to construct the structure of four ligands and optimizing the energy. Amber was used to make force field parameters and autodock vina was used to conduct docking experiment. The results were shown in **Fig 6**. There are two loops (Asp147, Ala170) in hTIR1, which served as binding sites for ligand recognition and form hydrogen bond with the amino/ imino group of the ligand. In addition, the phosphate groups in GMP and IMP interacted with Arg277's thiol group and bound to the amino group at Asn69 to form a hydrogen bond, which enabled the binding of VFT activity pocket to become more compact, it also explained GMP and IMP had a synergistic effect for umami taste.

In related researches, Wauson's demonstrated that T1R1/T1R3 was distributed in almost all tissues, organs and cells, suggesting that the receptor has a universal function[33]. In addition, the mammalian target of rapamycin complex 1(mTORC1), which plays an important regulatory role in protein synthesis and cell development, is an integrated nutritional information, particularly amino acid nutrition. When amino acid deficiency (starvation) occurs in the body, mTORC1 supplies amino acid raw materials for the synthesis of the most important proteins by activating autophagy. The researchers proved that T1R1/T1R3, as a collector of umami signals, can pass information on the amino acid status and availability of food to mTORC1. Moreover, interference to T1R1/T1R3 signaling can alter the localization of mTORC1 to cell. These findings demonstrate that T1R1/T1R3 as an amino acid sensor can cause communication between amino acid status and mTORC1, and T1R1/T1R3 signaling plays an important role in nitrogen source sensing, absorption, and metabolism.

The experimental results of this study showed the allosteric constants of T1R1 combined with four umami substances as follows: $K_{GMP}>K_{MSG}>K_{IMP}>K_{SUC}$. For their molecular structure, there is a bit difference on amino group (**Fig. 6**). The GMP and MSG (containing amino group) have a lower allosteric constant than the IMP and SUC, and GMP with a higher nitrogen content has a lower allosteric constant than MSG. Based on the above analysis, we believe that hT1R1 may be a receptor for sensing nitrogen signals in the body, and ligands containing amino groups are preferentially recognized.

In summary, umami receptor acts as the "eye" of the cell to identify the available amino acids (nitrogen sources) in the environment for absorption. As a nitrogen containing nutrient sensing receptor, this may be one of the reasons why umami receptors are present in all mammalian cells.

Fig. 6 Molecular docking diagram of ligands and hT1R1, the embedded diagram is molecular structure; a, b, c, d represents MSG, IMP, SUC, GMP, respectively.

4. Conclusions

Compared with other methods of determining receptor-ligand interactions, the detection platform constructed in this paper is based on the linkage between signal generation and amplification. The analysis of the kinetics showed that the of the hT1R1 for four umami substances was: GMP > MSG > IMP > SUC; Molecular simulation and structural analysis showed that hT1R1 may be a receptor of sensing "nitrogen" signal in the body, and the ligand containing amino group was preferentially recognized. The new discovery in this paper will contribute to the study of functional foods and nutrient absorption.

Conflicts of interest

There are no conflicts to declare.

Acknowledgements

This work was funded by National Natural Science Foundation of China (Grant No. 31622042, 31401571, 31371790, 31271900, 31671857) and The National Key R&D Program of China (2016YFD0400803, 2016YFD0401501).

Notes and references

1. K. Kurihara, Umami the Fifth Basic Taste: History of Studies on Receptor Mechanisms and Role as a Food Flavor, *Biomed Res Int*, 2015, **2015**, 189402.
2. J. Liu, K. Yu and W. Zhu, Amino acid sensing in the gut and its mediation in gut-brain signal transduction, *Animal Nutrition*, 2016, **2**, 69-73.
3. Eric M. Wauson, E. Zaganjor, A. Lee, Marcy L. Guerra, Anwesha B. Ghosh, Angie L. Bookout, Chris P. Chambers, A. Jivan, K. Mcglynn and Michele R. Hutchison, The G Protein-Coupled Taste Receptor T1R1/T1R3 Regulates mTORC1 and Autophagy, *Molecular Cell*, 2012, **47**, 851.
4. R. J. Lee and N. A. Cohen, Taste receptors in innate immunity, *Cell Mol Life Sci*, 2015, **72**, 217-236.
5. E. Rozengurt and C. Sternini, Taste receptor signaling in the mammalian gut, *Curr Opin Pharmacol*, 2007, **7**, 557-562.
6. S. S. Calvo and J. M. Egan, The endocrinology of taste receptors, *Nat Rev Endocrinol*, 2015, **11**, 213-227.

7. N. Nuemket, N. Yasui, Y. Kusakabe, Y. Nomura, N. Atsumi, S. Akiyama, E. Nango, Y. Kato, M. K. Kaneko, J. Takagi, M. Hosotani and A. Yamashita, Structural basis for perception of diverse chemical substances by T1r taste receptors, *Nat Commun*, 2017, **8**, 15530.
8. B. K. Feng Zhanga, Richard M. Fineb, Hong Xua, Alexey Pronina, Haitian Liua, Catherine Tachdjiana, and Xiaodong Lia,1, Molecular mechanism for the umami taste synergism, *PNAS*, 2008, **105**.
9. Y. Dang, X. Gao, A. Xie, X. Wu and F. Ma, Interaction between umami peptide and taste receptor T1R1/T1R3, *Cell Biochem Biophys*, 2014, **70**, 1841-1848.
10. X. Yu, L. Zhang, X. Miao, Y. Li and Y. Liu, The structure features of umami hexapeptides for the T1R1/T1R3 receptor, *Food Chem*, 2017, **221**, 599-605.
11. I. Navratilova, J. Besnard and A. L. Hopkins, Screening for GPCR Ligands Using Surface Plasmon Resonance, *Acs Med Chem Lett*, 2011, **2**, 549-554.
12. C. S. Wu, L. P. Du, L. Zou, L. H. Zhao, L. Q. Huang and P. Wang, Recent advances in taste cell- and receptor-based biosensors, *Sensor Actuat B-Chem*, 2014, **201**, 75-85.
13. H. S. Song, H. J. Jin, S. R. Ahn, D. Kim, S. H. Lee, U. K. Kim, C. T. Simons, S. Hong and T. H. Park, Bioelectronic Tongue Using Heterodimeric Human Taste Receptor for the Discrimination of Sweeteners with Human-like Performance, *Acs Nano*, 2014, **8**, 9781-9789.
14. M. Lee, J. W. Jung, D. Kim, Y. J. Ahn, S. Hong and H. W. Kwon, Discrimination of Umami Tastants Using Floating Electrode-Based Bioelectronic Tongue Mimicking Insect Taste Systems, *Acs Nano*, 2015, **9**, 11728-11736.
15. P. Rondard, C. Goudet, J. Kniazeff, J. P. Pin and L. Prézeau, The complexity of their activation mechanism opens new possibilities for the modulation of mGlu and GABA B class C G protein-coupled receptors, *Neuropharmacology*, 2011, **60**, 82-92.
16. Z. Qin, B. Zhang, K. Q. Gao, L. J. Zhuang, N. Hu and P. Wang, A whole animal-based biosensor for fast detection of bitter compounds using extracellular potentials in rat gustatory cortex, *Sensor Actuat B-Chem*, 2017, **239**, 746-753.
17. Z. Qin, B. Zhang, L. Hu, L. J. Zhuang, N. Hu and P. Wang, A novel bioelectronic tongue in vivo for highly sensitive bitterness detection with brain-machine interface, *Biosensors & Bioelectronics*, 2016, **78**, 374-380.
18. D. Q. Lu, F. P. Lu, L. H. Geng and G. C. Pang, Recent Advances in Olfactory Receptor Biosensors and Cell Signaling Cascade Amplification Systems, *Sensor Mater*, 2018, **30**, 67-87.
19. L. Wei, X. Wang, D. Lu, Y. Li, G. Pang and J. Xie, A Novel Staphylococcal Enterotoxin Q Immunosensor Prepared with Self-Assembly Method Based on Horseradish Peroxidase and Double-Layer Gold Nanoparticles, *Food Analytical Methods*, 2016, **10**, 892-899.
20. D. Q. Lu, F. P. Lu and G. C. Pang, A novel glutathione-S transferase immunosensor based on horseradish peroxidase and double-layer gold nanoparticles, *Biomed Microdevices*, 2016, **18**.
21. D. Lu, F. Lu and G. Pang, A Novel Tetrahydrocannabinol Electrochemical Nano Immunosensor Based on Horseradish Peroxidase and Double-Layer Gold Nanoparticles, *Molecules*, 2016, **21**.
22. X. B. Kang, G. C. Pang, Q. S. Chen and X. Y. Liang, Fabrication of Bacillus cereus electrochemical immunosensor based on double-layer gold nanoparticles and chitosan, *Sensor Actuat B-Chem*, 2013, **177**, 1010-1016.
23. X. B. Kang, G. C. Pang, X. Y. Liang, M. Wang, J. Liu and W. M. Zhu, Study on a hydrogen peroxide biosensor based on horseradish peroxidase/GNPs-thionine/chitosan, *Electrochimica Acta*, 2012, **62**, 327-334.
24. A. J. Venkatakrishnan, X. Deupi, G. Lebon, C. G. Tate, G. F. Schertler and M. M. Babu, Molecular signatures of G-protein-coupled receptors, *Nature*, 2013, **494**, 185-194.
25. S. R. Ahn, J. H. An, H. S. Song, J. W. Park, S. H. Lee, J. H. Kim, J. Jang and T. H. Park, Duplex Bioelectronic Tongue for Sensing Umami and Sweet Tastes Based on Human Taste Receptor Nanovesicles, *Acs Nano*, 2016, **10**, 7287-7296.
26. K. Omidfar, H. Zarei, F. Gholizadeh and B. Larijani, A high-sensitivity electrochemical immunosensor based on mobile crystalline material-41-polyvinyl alcohol nanocomposite and colloidal gold nanoparticles, *Anal Biochem*, 2012, **421**, 649-656.
27. L. H. Wei, L. X. Qiao, G. C. Pang and J. B. Xie, A kinetic study of bitter taste receptor sensing using immobilized porcine taste bud tissues, *Biosensors & Bioelectronics*, 2017, **92**, 74-80.
28. L. Qiao, L. Jiao, G. Pang and J. Xie, A novel pungency biosensor prepared with fixing taste-bud tissue of rats, *Biosens Bioelectron*, 2015, **68**, 454-461.
29. D. M. Zhang, F. N. Zhang, Q. Zhang, Y. L. Lu, Q. J. Liu and P. Wang, Umami evaluation in taste epithelium on microelectrode array by extracellular electrophysiological recording, *Biochem Bioph Res Co*, 2013, **438**, 334-339.
30. S. R. Ahn, J. H. An, I. H. Jang, W. Na, H. Yang, K. H. Cho, S. H. Lee, H. S. Song, J. Jang and T. H. Park, High-performance bioelectronic tongue using ligand binding domain T1R1 VFT for umami taste detection, *Biosensors & Bioelectronics*, 2018, **117**, 628-636.
31. L. Lu, X. Hu and Z. Zhu, Biomimetic sensors and biosensors for qualitative and quantitative analyses of five basic tastes, *TrAC Trends in Analytical Chemistry*, 2017, **87**, 58-70.
32. D. Ha, Q. Sun, K. Su, H. Wan, H. Li, N. Xu, F. Sun, L. Zhuang, N. Hu and P. Wang, Recent achievements in electronic tongue and bioelectronic tongue as taste sensors, *Sensors and Actuators B: Chemical*, 2015, **207**, 1136-1146.
33. E. M. Wauson, E. Zaganjor, A. Y. Lee, M. L. Guerra, A. B. Ghosh, A. L. Bookout, C. P. Chambers, A. Jivan, K. McGlynn, M. R. Hutchison, R. J. Deberardinis and M. H. Cobb, The G Protein-Coupled Taste Receptor T1R1/T1R3 Regulates mTORC1 and Autophagy, *Molecular Cell*, 2012, **47**, 851-862.

Fig. 1

View Article Online
DOI: 10.1039/C8FO02522C

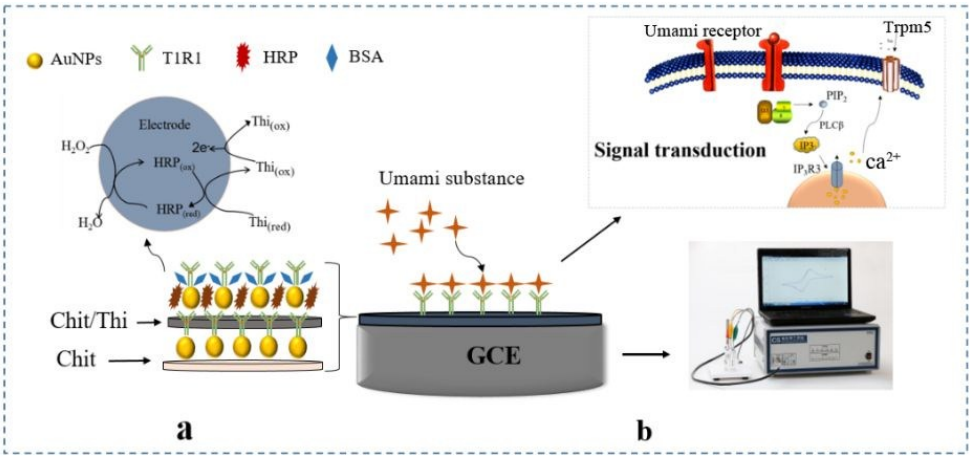

Fig. 2

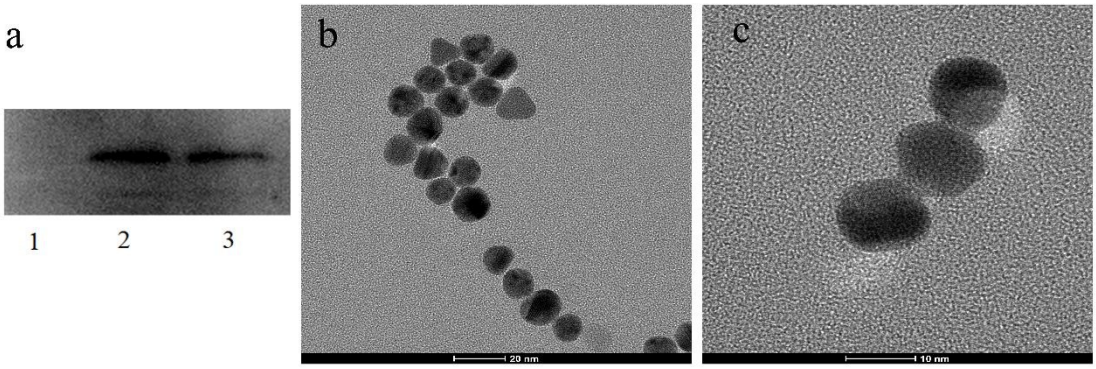

Fig. 3

View Article Online
DOI: 10.1039/C8FO02522C

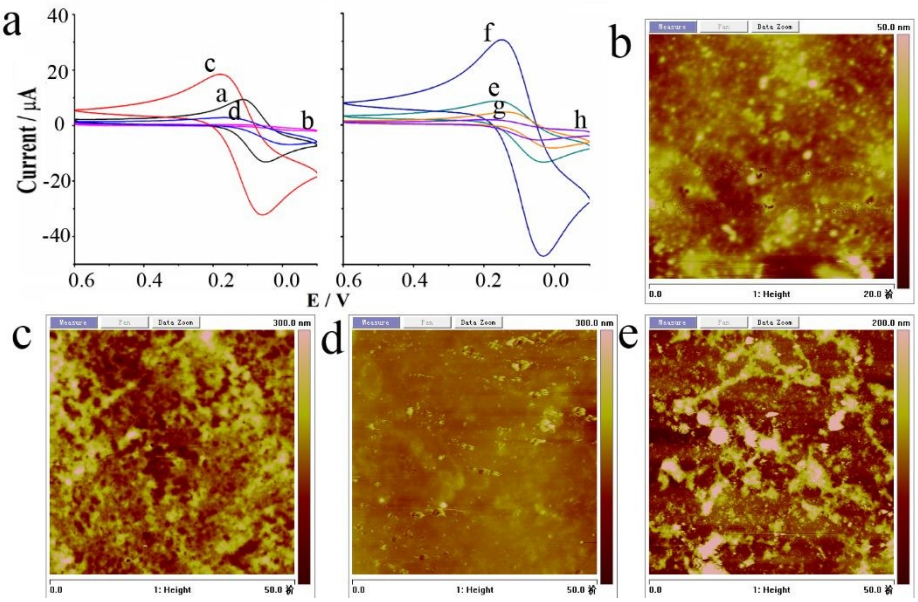

Fig. 4

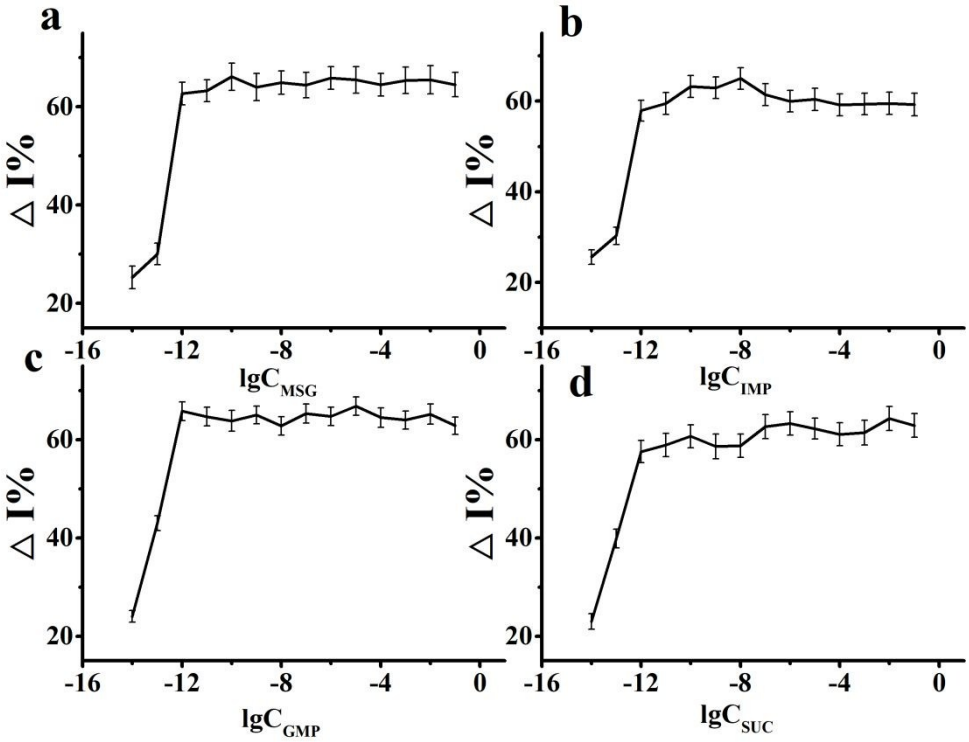

View Article Online
DOI: 10.1039/C8FO02522C

Fig. 5

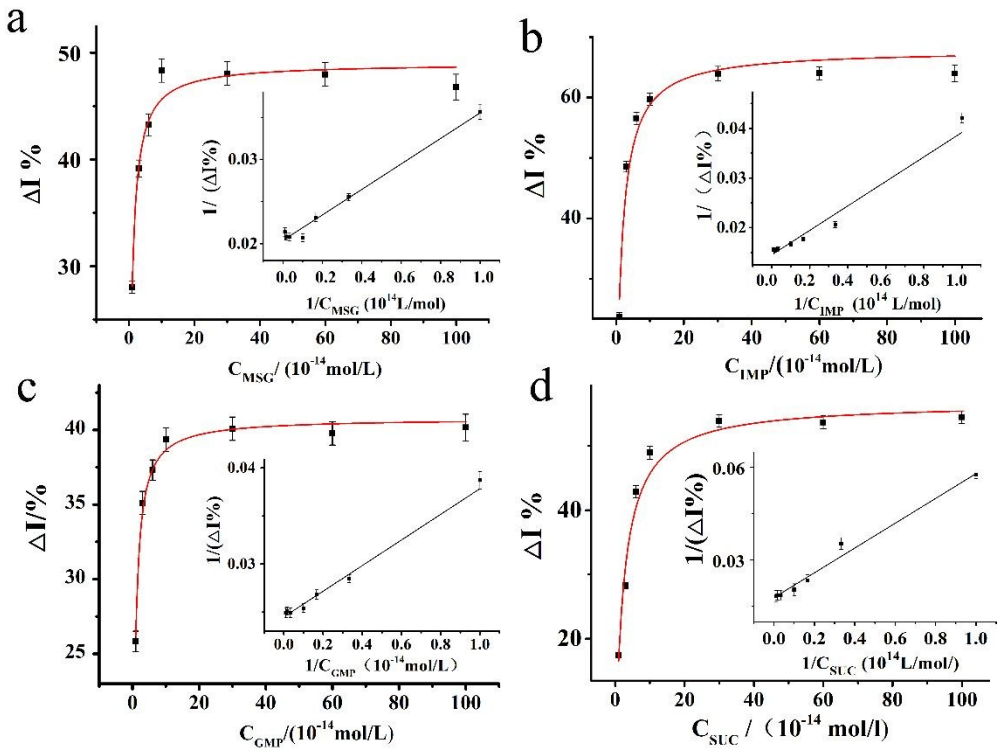

Fig. 6

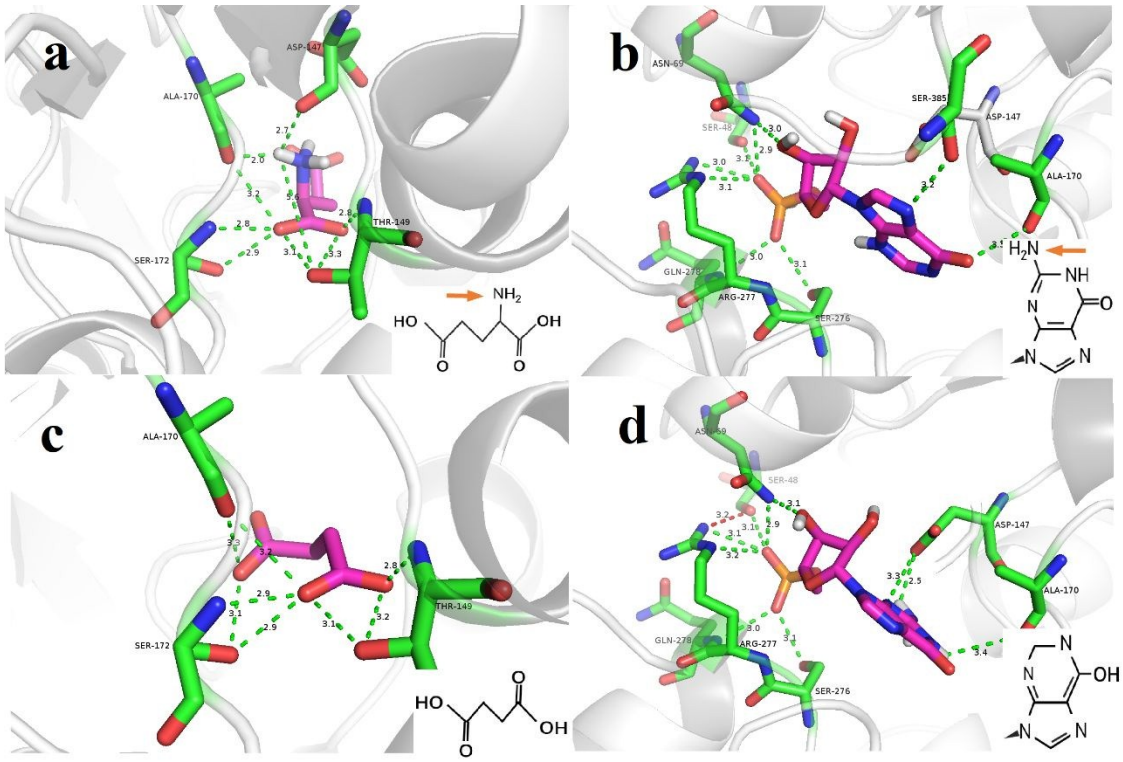

Journal Name ARTICLE

View Article Online
DOI: 10.1039/C8FO02522C

Table 1

Table 1 Surface roughness, peak height and peak spacing during electrode assembly

Assembly steps	Ra Value (nm)	peak depth (nm)	Peak to peak distance (nm)
f	5.68	72.5	1.58
g	35.7	295	1.91
h	10.1	221	1.07
i	35.8	588	4.35

DOI: 10.1039/C8FO02522C

The biosensor reflects the linkage of the umami signal during conduction and amplification, and study on receptor-ligand recognition mechanism.